

## Development of P(VDF-Trfe) Films and Its Quasi-Static and Dynamic Strain Response

Anjana Jain<sup>\*1</sup>, S. Jayanth Kumar<sup>1</sup>, D. Roy Mahapatra<sup>2</sup>, V. T. Rathod<sup>2</sup>

<sup>1</sup> Materials Science Division, National Aerospace Laboratories, Bangalore, India

<sup>2</sup> Department of Aerospace Engineering, Indian Institute of Science, Bangalore, India

### Abstract

Thin films of poly(vinylidene fluoride-trifluoroethylene) P(VDF-TrFE) were prepared using solvent cast method and characterized for structural, mechanical and surface morphological properties to investigate the presence of  $\beta$ -phase through X-ray diffraction, scanning electron microscopy, differential scanning calorimeter, Raman and Infrared spectra, and tensile testing. The conditions to achieve  $\beta$ -phase of P(VDF-TrFE) have been discussed in detail. Following the material characterization, the fabricated  $\beta$ -phase P(VDF-TrFE) sensors have been tested for dynamic strain sensing application. Time response from the  $\beta$ -phase P(VDF-TrFE) sensor due to the free vibration and impact on beam structure is obtained and is compared with  $\beta$ -phase PVDF sensor and conventional piezoelectric wafer type sensor. The variations in the frequency response spectra due to free vibration and impact loading conditions are also reported, which reveal the fact that the sensitivity of the  $\beta$ -phase P(VDF-TrFE) sensor to various modes of vibration is same as the  $\beta$ -phase PVDF sensor. The resonant and anti-resonant peaks in the frequency response of  $\beta$ -phase P(VDF-TrFE) films match well with that of  $\beta$ -phase PVDF sensor and Lead zirconate titanate (PZT) wafer sensors. Thus the fabricated  $\beta$ -phase P(VDF-TrFE) sensors can be effectively used as the dynamic strain sensor.

**Keywords:** P(VDF-TrFE), piezoelectricity, sensors, X-ray diffraction.

### 1. Introduction

Uniaxially oriented polyvinylidene fluoride (PVDF) is well known to exhibit appreciable ferroelectric, piezoelectric and pyroelectric behaviour [1-3]. In addition copolymers of vinylidene fluoride with other ferroelectric polymers also show significant electro active response [4]. P(VDF-TrFE) crystallizes into various crystal forms depending on their molar content

ratios of VDF (x) and TrFE (1-x), and on crystallization conditions [5]. P(VDF-TrFE) shows excellent ferroelectric and piezoelectric properties for composition range of 55 to 85 mole% vinylidene fluoride content [6] and have essentially a similar structure and confirmation as PVDF but with larger lattice parameters in the crystal a-b plane due to the extra fluorine atom on the TrFE monomers [7-9]. These copolymers also show increase in the Curie transition temperature as the vinylidene fluoride content increases [10]. They crystallize from the melt into a crystal form analogous to the polar phase I or  $\beta$ -phase of PVDF, characterized by an all-trans confirmation of the polymer chains, pseudo-hexagonal chain packaging and a polar unit cell. Therefore these polymers do not need stretching before poling [5].

It has tremendous applications in electronic industry, such as soft transducers, infrared imaging, and compact capacitors and holds a promising future in the field of non-volatile memory [11]. It also finds many applications in electromechanical devices, to perform energy conversion between the electric and mechanical forms such as artificial muscles, smart skins for drag reduction, actuators for active noise and vibration controls, and micro-fluidic systems for drug delivery and micro-reactors [12]. One of the most unique applications of P(VDF-TrFE) is their utilization as active piezoelectric elements in self-powered, nanosecond time-resolved, dynamic stress gauges for the study of shock-wave compression phenomena [13, 14]. The films made by the Langmuir-Blodgett (LB) method are polycrystalline with chains parallel to the film, as revealed by X-ray diffraction and polarized infrared spectra, and seem to be without lamellar structure [15]. X-ray diffraction studies [16] showed that the films in ferroelectric phase ( $\beta$ -phase) with all-trans conformation have (110) orientation. V. Sencadas et al. studied the phase transition and piezoelectric properties of P(VDF-TrFE) [17]. Further, Li et al [18] reported the combination of P(VDF-TrFE) has been applicable to transducers, sensors, actuators, and high-density memories. But its electron emission capability

under an applied field has been ignored. In this paper, thin films of P(VDF-TrFE) were prepared by solvent cast method and are characterized for structural, mechanical, surface and piezoelectric properties. The presence of  $\beta$ -phase is established by comparing the properties of films of  $\beta$ -phase PVDF polymer with those of P(VDF-TrFE) films. The performance of P(VDF-TrFE) films has also been evaluated by recording the vibration modes of cantilever beam and by comparing the response with that of PVDF and PZT wafer sensor.

## 2. Experiment details

The pellets of PVDF (Fig. 1a) were procured from Pennwalt India Ltd and PTrFE polytrifluoroethylene (Fig. 1b) were procured from Nikunj Eximp Enterprises India Pvt Ltd. The films of  $\sim 100$  micrometer thickness were prepared using solvent cast method. PVDF and PTrFE were taken in the compositions of 80/20 mol%. Saturated solution of P(VDF-TrFE) is formed by dissolving pellets in dimethyl formamide and were cast on to a glass plate. The solution is evaporated in an oven to obtain a  $\beta$ -phase P(VDF-TrFE) film.

## 3. Characterization of P(VDF-TrFE) films

P(VDF-TrFE) are known to exhibit higher electro activity than that of PVDF homopolymer due to higher abundance of the polymer all-trans conformation. Diffraction patterns were recorded with Rigaku D/max Ultima 2200 X-ray diffractometer using  $\text{CuK}\alpha$  radiation with graphite monochromator to identify the phase. The indexing was done using unit cell dimensions of  $a=8.82$ ,  $b=5.13$ ,  $c=2.55$ , reported by Duo Mao et al [19]. Surface features of the films were examined using a Jeol scanning electron microscope. Raman spectrum is recorded by Labram Spectrometer in the wave number range of 700-1100 $\text{cm}^{-1}$ . Laser power of  $\sim 20\text{mW}$  was obtained from a He-Ne laser, and Infrared spectrum was recorded with Bruker Vector spectrometer. Differential Scanning Calorimetric measurements were conducted with a DSC-2920 to evaluate the degree of crystallinity. The samples were subjected to temperatures ranging from 110-200 $^{\circ}\text{C}$ , at a constant heating rate of 10 $^{\circ}\text{C}/\text{min}$  under nitrogen atmosphere. Tensile properties of the film were measured using INSTRON 5500. The test specimens, 15cm long and 1cm wide, were cut from the  $\beta$ -phase films and clamped on to the grips of the machine with the help of rubber pads to avoid slippage or damage at the grips during the experiments. Load was increased to achieve a strain rate of 10mm/min till the failure limit of the specimen is reached.

The  $\beta$ -phase films were electroded with silver paste and poled by thermal contact method at an electric field of

75 kV/mm. This aligns the dipoles in the crystalline regions in the field direction. Subsequent cooling to room temperature under the applied field stabilizes the polar alignment resulting in permanent polarization.

## 4. Results and discussion

Fig. 2 shows the P(VDF-TrFE) film with thickness  $\sim 100\mu\text{m}$  obtained from solvent cast technique from PVDF and PTrFE pellets.

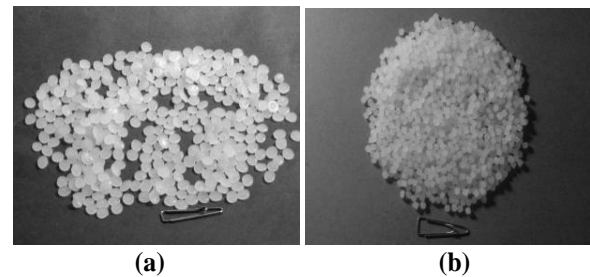


Fig. 1 (a) PVDF Pellets, (b) PTrFE Pellets

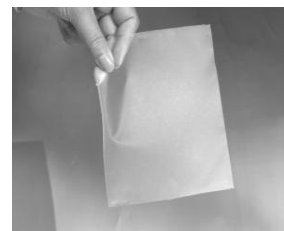


Fig. 2 P(VDF-TrFE) film

### 4.1 X-Ray diffraction

Fig. 3 shows the X-ray diffraction of P(VDF-TrFE) film prepared by solvent cast method

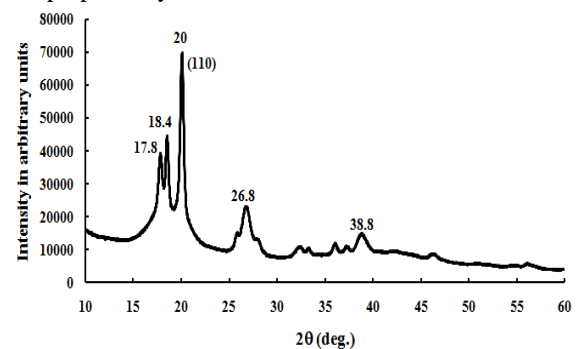


Fig. 3 XRD pattern of P(VDF-TrFE) film

From the XRD pattern of P(VDF-TrFE), it is seen that the most intense reflection (110) of  $\beta$ -phase occurs at  $2\theta = 20^{\circ}$ , which is in agreement with the value ( $2\theta = 20^{\circ}$ ) calculated from the unit cell dimensions given by Duo Mao et al [19]. Apart from  $2\theta = 20^{\circ}$ , peaks were also observed at  $2\theta$  values of 18.4 $^{\circ}$  and 17.8 $^{\circ}$ . This is consistent with the earlier observations of unstretched films exhibiting multiple peaks [20]. The probable

cause, as reported, for these peaks were hexagonal packing of 3/1-helical chains generated due to the presence of TG and TG' defects and similarly packed trans-planar chains.

From the XRD pattern, the crystallite size and micro strains were calculated using  $2\theta$ , full width at half maxima and intensity values [21]. It was found that crystallite size (coherently scattering domain size) = 23.86 nm and micro strain = 0.0075 for P(VDF-TrFE) films.

#### 4.2 Film microstructure

The micrographs features of  $\alpha$ - and  $\beta$ -phase PVDF films are shown in the Fig. 4a, and 4b. The  $\alpha$ -phase film shows grain-like features measuring  $\sim 50 \mu\text{m}$ . The grain-like features disappear after hot-stretching the  $\alpha$ -phase films as the PVDF film transforms to polar  $\beta$ -phase; surface shows oriented fibril-like structure [22]. Due to the long molecular chain structure of polymeric materials, a fully crystalline state is usually hard to obtain. This is consistent with the XRD and IR results. The molecular arrangement in P(VDF-TrFE) film is such that it is in  $\beta$ -phase without mechanical stretching. The surface features of the PVDF films shows that grain-like features which are observed in  $\alpha$ -phase, are not seen in P(VDF-TrFE) films. The similar features have been observed earlier by several investigators [23, 24]. Unlike the homopolymer PVDF, P(VDF-TrFE) does not require stretching to generate a polar crystalline phase.

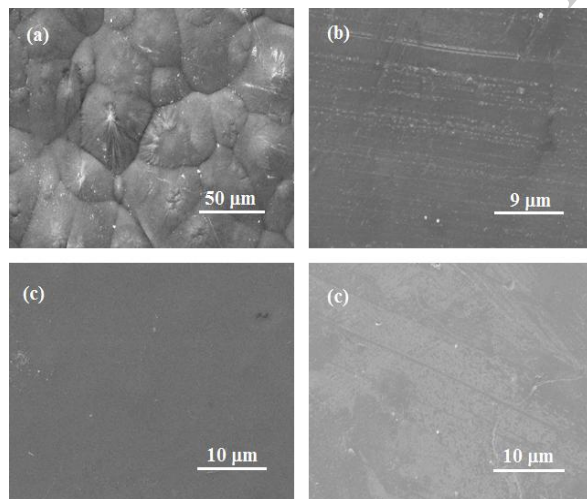


**Fig. 4 SEM surface scans: (a) PVDF  $\alpha$ -phase film; (b) PVDF  $\beta$ -phase film; (c) P(VDF-TrFE)  $\beta$ -phase film**

#### 4.3 Infrared spectroscopy

Phase transitions in the P(VDF-TrFE) films were also reflected by the molecular conformational change. Detailed interpretation of the vibrational spectra of PVDF and its copolymers with various crystalline modifications enables the reasonable assignment of the absorption bands to the characteristic sequences of Trans and Gauche states [25, 26-28]. The Infrared spectroscopy measurements were carried out in order to investigate the changes in the copolymer due to the presence of  $\beta$ -phase. Fig. 5 shows the Infrared spectra of P(VDF-TrFE) in the  $400\text{-}1200 \text{ cm}^{-1}$  region. Although, there are several peaks for each type of copolymer conformation, the obtained spectra represent the  $\beta$ -phase at the bands marked 473, 505, 614, 845, 882, 1078, and  $1107 \text{ cm}^{-1}$ , which corresponds to the presence of all-trans ferroelectric  $\beta$ -phase of P(VDF-TrFE) [29, 30]. No indication for alternating trans-gauche conformation is observed.

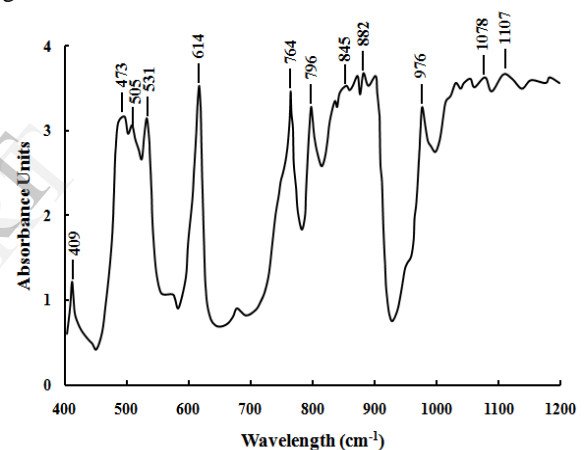


**Fig. 5 IR Spectra of PVDF-TrFE film**

#### 4.4 Raman spectroscopy

Fig. 6 shows the Raman spectra of  $\beta$ -phase P(VDF-TrFE) film. It is clear from the pattern that the Raman bands were found to be at  $754.2$  (very strong band B2, CH<sub>2</sub> rocking),  $872.7$  (B2, CH<sub>2</sub> rocking),  $1053 \text{ cm}^{-1}$  (B2, CF<sub>2</sub> Antisymmetric stretching), corresponds to  $\beta$ -phase of P(VDF-TrFE) film [31].

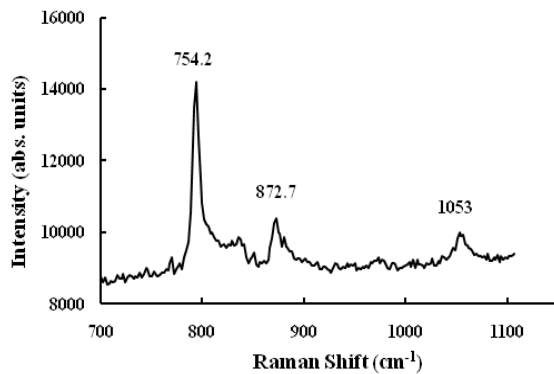


Fig. 6 Raman Spectrum of P(VDF-TrFE) film

#### 4.5 Differential scanning calorimeter (DSC)

The correct temperature for annealing and poling was chosen only after a careful investigation of the transition temperatures. DSC was used to characterize phase transitions of the P(VDF-TrFE) film and the results are shown in (Fig. 7).

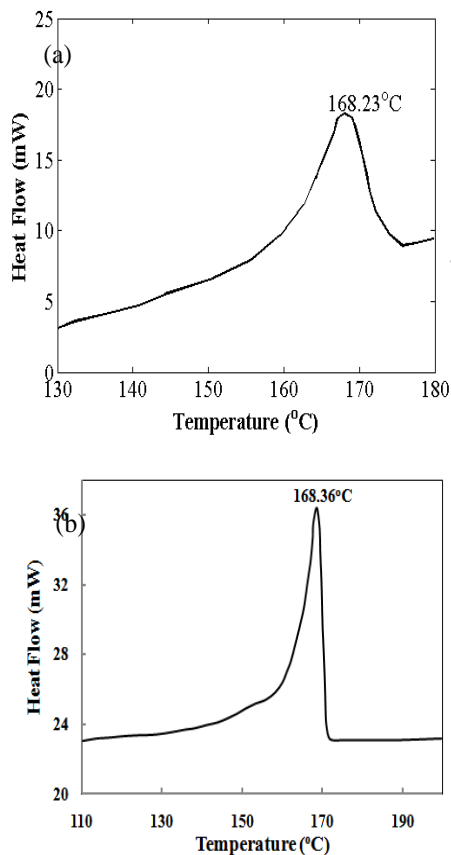


Fig. 7 DSC curves: (a)  $\beta$ -phase PVDF films (b)  $\beta$ -P(VDF-TrFE) film

Fig. 7a and 7b shows typical DSC traces for the  $\beta$ -phase of PVDF and PVDF-TrFE films. The melting

peak occurs at 168.23°C for the  $\beta$ -PVDF and 168.36°C for the  $\beta$ -P(VDF-TrFE). The marginally higher density of the  $\beta$ -P(VDF-TrFE) (Table 2) reflects in the higher melting point on the DSC curves. The films in both  $\alpha$ - and  $\beta$ -phases contain substantial fraction of the amorphous phase. One of the methods to estimate the degree of crystallinity is to use the enthalpy of the melting peak obtained from DSC scans [17]. The degree of crystallinity  $\Delta X_c$  is given by,

$$\Delta X_c = \left( \frac{\Delta H_f}{\Delta H_{100}} \right) \times 100 \quad (1)$$

In Eq. (1),  $\Delta H_f$  is the enthalpy of the melting peak  $\Delta H_{100}$  and is enthalpy of the fully crystallized PVDF. Similarly, the degree of crystallinity of the P(VDF-TrFE) was calculated according to the following equation of Eq. (2):

$$\Delta X_c = \left( \frac{\Delta H_m}{(\Delta H_m^o)_{P(VDF-TrFE)}} \right) \times Wt\%_{P(VDF-TrFE)} \quad (2)$$

Where  $\Delta H_m$  and  $Wt\%_{P(VDF-TrFE)}$  are, respectively, the apparent melting enthalpy and the weight fraction of P(VDF-TrFE) in the composites and  $\Delta H_m^o$ , P(VDF-TrFE) is the value of enthalpy corresponding to a 100% crystalline P(VDF-TrFE) (80/20) copolymer, taken as 91.45 J/g [31, 32,33].

#### 4.6 Tensile properties

Studies on the deformation and fracture mechanisms under pure or combined mechanical and electric loads can help to better understand the electromechanical coupling effects in the P(VDF-TrFE) film. The films are subjected to standard tensile tests in the Instron testing machine and the tensile properties of PVDF and P(VDF-TrFE) films are determined.

The literature value [34-36] of Young's modulus (2-2.5 GPa), tensile strength (35-50 MPa) of PVDF show a considerable spread. The major factors contributing to this spread are different crystalline-to-amorphous ratio and porosity in the specimens. The present values are measured on P(VDF-TrFE) thin films. It is found that young's modulus was found to be 2.24 GPa for PVDF and 4.89 GPa for P(VDF-TrFE) and tensile stress as 244 MPa for PVDF and 44.19 MPa for P(VDF-TrFE) (Table 1). The properties of PVDF were compared with those of P(VDF-TrFE) films in Table 2 [37].

**Table 1 Mechanical properties of  $\beta$ -phase PVDF and P(VDF-TrFE) films**

Sample	Modulus (Young's -Cursor) (GPa)	Extension at Maximum Tensile extension (mm)	Maximum Load (N)	Tensile stress at Maximum Load (MPa)
PVDF	2.24	18.6	98.53	244
P(VDF-TrFE)	4.89	5.0	64.90	44.19

**Table 2 Comparison between PVDF and P(VDF-TrFE) film**

Parameter	PVDF	P(VDF-TrFE)
Relative Dielectric Const. $\epsilon_r = \epsilon/\epsilon_0$	12	7
Piezoelectric Charge Const. $d_{33}$ (pC/N)	33	38
Piezoelectric Voltage Const. $g_{33}$ ( $10^{-3}$ Vm/N)	330	542
Acoustic Impedance $Z$ ( $10^6$ kg/m <sup>2</sup> s)	4.02	4.49
Young's Modules ( $10^9$ N/m <sup>2</sup> )	2-2.5	5
Electromechanical Coupling Factor	0.205	0.292
Capacitance (pF/cm <sup>2</sup> )	380 for 28 $\mu$ m	68 for 100 $\mu$ m
Density ( $10^3$ kg/m)	1.78	1.82
Tangent Loss	0.02	0.015
Yield Strength ( $10^6$ N/m <sup>2</sup> )	45	20

#### 4.7 Sensitivity to mechanical vibration and impact

In previous sections, the  $\beta$ -phase P(VDF-TrFE) films are characterized for material properties. In this section, the performance of the  $\beta$ -phase P(VDF-TrFE) film in sensing the dynamic strain is studied. The  $\beta$ -phase P(VDF-TrFE) film is subjected to dynamic strains induced due to the free vibration and transient impact loading on a beam structure, as done in [38]. The cantilever setup with the  $\beta$ -phase P(VDF-TrFE) film bonded at the root of the cantilever is shown in Fig. 8.

The material of the beam structure is aluminium. The beam has a length, width and thickness of 0.3m, 0.025m and 0.002m respectively. Identical operating conditions are ensured between the  $\beta$ -phase P(VDF-TrFE) film and the other two types sensors considered for comparison, by preparing three identical cantilever beam specimens and bonding the sensors at identical locations, at the root of the cantilever. During the impact or free vibration testing, the sensors are connected to the Data Acquisition System (DAQ), run by lab VIEW as a virtual controller. First the sensitivity of the bonded  $\beta$ -phase P(VDF-TrFE) film to the dynamic strains induced from the free vibration of the beam structure is studied. The beam is given an initial displacement and left it to vibrate on its own, inducing the free vibrations. During the free vibration of the beam structure, the voltage response of the P(VDF-TrFE) film was recorded using a DAQ. The free vibrations are induced in the beam structures in a similar way and the voltage responses from the PVDF film and PZT-5H wafer sensor are recorded for comparison. The voltage responses are normalized with the thickness for the three types of sensors and are compared. This normalization eliminates the variations in the voltage response due to the difference in thickness of the sensors. A close matching of the waveform of the voltage responses for the three sensors are seen in Fig. 9(a). The magnitude of the voltage response of the P(VDF-TrFE) film is almost the same as that of the PVDF film sensor with a small difference of 8%. Thus, the sensitivity of the P(VDF-TrFE) film is almost same to that of the PVDF film sensor and the PZT wafer. Using the Fast Fourier Transform (FFT) of the normalized voltage history, the frequency response was obtained as shown in Fig. 9(b). The peaks reveal the resonance frequencies of various different modes of vibration of the cantilever beam. The peaks as well as the mean levels captured by the P(VDF-TrFE) film sensor are in good agreement and show comparable sensitivities with the PVDF film sensor and PZT wafer sensor.

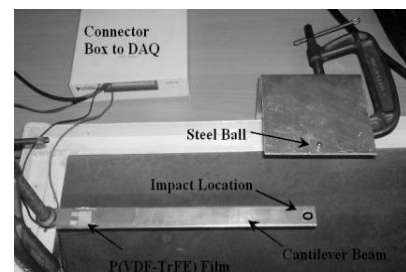


**Fig. 8 Experimental setup showing a cantilever beam with P(VDF-TrFE) film bonded on it, for free vibration and impact testing**

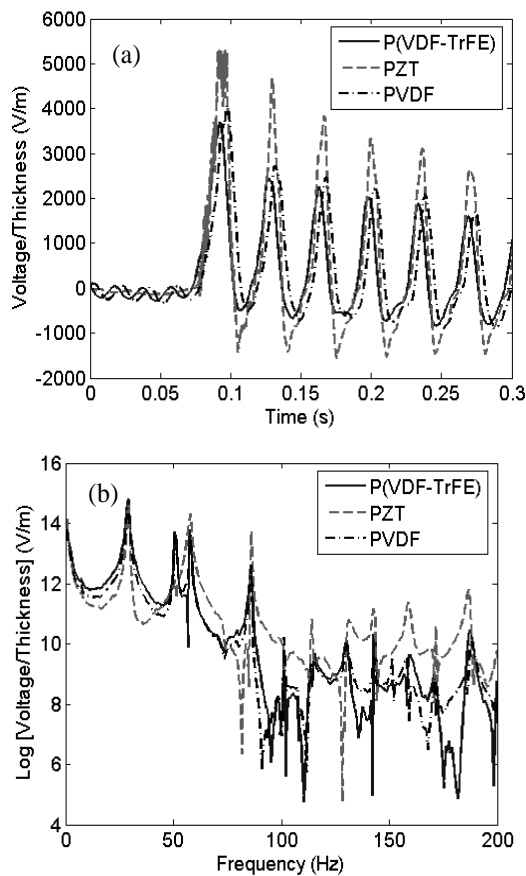


**Fig. 9 Comparison of the response of P(VDF-TrFE) film, PVDF film and PZT wafer sensors subjected to the dynamic strains induced due to free vibration:**

**(a) Voltage response (b) Frequency response**

Having compared the responses of the P(VDF-TrFE) film, PVDF film and PZT wafer sensors for free vibration, the response for an impact is compared here. Response of the P(VDF-TrFE) film sensor to the dynamic strains induced by an impact loading is studied by dropping a steel ball at the tip of the beam structure from a known height, as shown in Fig. 8. A steel ball of diameter  $d = 0.0045\text{ m}$  was dropped from a height of  $h = 0.01\text{ m}$  at the tip of the cantilever beam. During the event of an impact, the steel ball hits the beam tip and falls off with negligible rebound of 1-2 mm. Neglecting the energy of rebound, the magnitude of impact in terms of energy in this case is found to be  $E = mgh = 3.74 \times 10^{-5}\text{ N-m}$ . Response of the P(VDF-TrFE) film, PVDF film and PZT wafer sensors for an impact type of loading are compared in Fig. 10(a). The responses have similar waveforms. The frequency responses obtained by taking the FFT of the sensor signals are compared in Fig. 10(b). The frequency response of the P(VDF-TrFE) is comparable to that of the response of the PVDF film and PZT wafer sensors.

Thus, the peaks in the frequency response representing different natural frequencies of the beam are effectively captured by the P(VDF-TrFE) film sensor like the standard PZT wafer sensor. The additional peaks in the response of the P(VDF-TrFE) film and PVDF film indicates the sensitivity to the additional modes of vibration of the beam. The sensitivity to additional modes is also seen in the similar studies done on PVDF film earlier in Ref. [38].

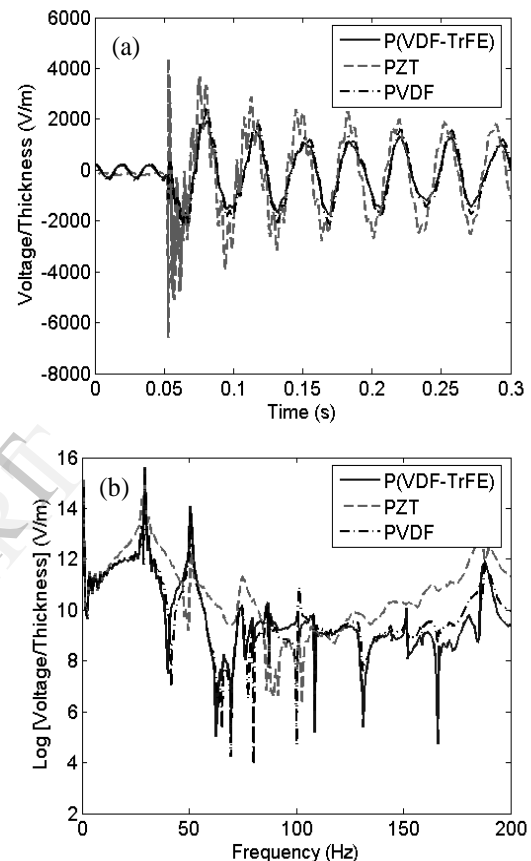


**Fig 10 Comparison of the response of P(VDF-TrFE) film, PVDF film and PZT wafer sensors subjected to the dynamic strains induced due to impact of magnitude  $3.74 \times 10^{-5}\text{ N-m}$  at the cantilever tip: (a) Voltage response (b) Frequency response**

Sensitivity to the different magnitudes of dynamic strains is studied by impacting the cantilever beam with a steel ball from different heights by adjusting the length of the frame (See Fig. 8). Two different magnitudes of impact are obtained by dropping the steel ball from a height of 0.01 m and 0.02 m to give the impact magnitude of  $3.74 \times 10^{-5}\text{ N-m}$  and  $7.49 \times 10^{-5}\text{ N-m}$  respectively.

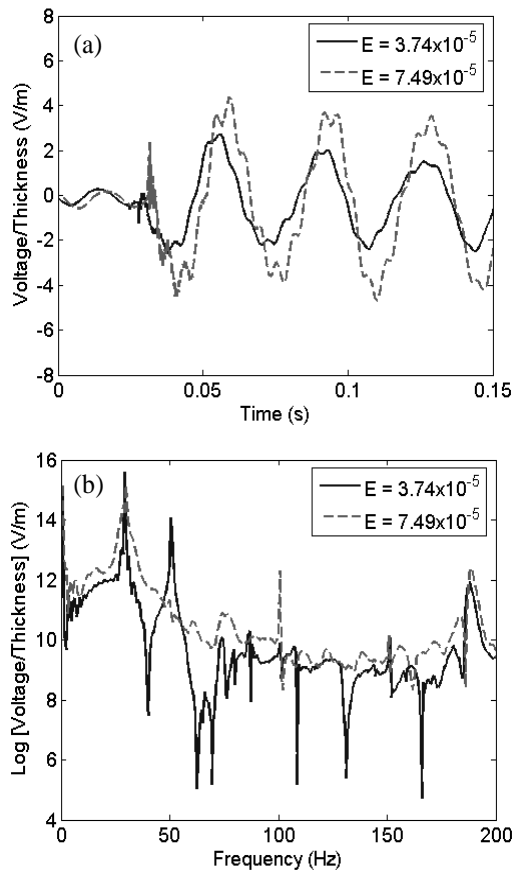


**Fig. 11 Comparison of the response of P(VDF-TrFE) film subjected to the dynamic strains induced due to different impact magnitudes at the cantilever tip: (a) Voltage response (b) Frequency response**

The response of the P(VDF-TrFE) sensor to different levels of impact is compared with the response of PVDF film and the PZT wafer as shown in Fig. 11(a). The peak voltage in the P(VDF-TrFE) sensor response for higher magnitude of impact is found to be higher than the peak voltage for a lower magnitude of impact. This shows that the P(VDF-TrFE) sensor is sensitive to the varying levels of dynamic strains. Fast Fourier transform of the voltage response of the P(VDF-TrFE) film shows the presence of additional modes in higher frequency range in case of impact event with higher magnitude. Except at a few resonant peaks, the frequency response is different for both the magnitude of impacts (Fig. 11b). Due to the sensitivity of the P(VDF-TrFE) film sensor to the additional modes of vibration, the P(VDF-TrFE) film sensor can be used more effectively in the quasi-static and dynamic strain sensing applications.

## 5. Conclusions

The P(VDF-TrFE) films were prepared using solvent cast method. The X-ray diffraction analysis shows that as-prepared films were in  $\beta$ -phase. The surface feature shows that by adding TrFE it directly transforms to  $\beta$ -phase. Raman and Infrared spectrum further confirms the presence of  $\beta$ -phase. The DSC scans indicated the higher melting point of P(VDF-TrFE) due to its higher density. Tensile properties were in agreement with those reported in literature. The sensitivity of the P(VDF-TrFE) film sensor to the dynamic strains induced due to the free vibration and impact is comparable to the sensitivity of the PVDF film and PZT wafer sensors. Thus, the P(VDF-TrFE) film sensor can be effectively used in the quasi-static and dynamic strain sensing applications.

## Acknowledgement

The authors thank the financial support provided by CSIR and NPMAS to carry out this project. The authors also thank Mr. Shyam Chetty, Director, NAL, Dr. A. R. Upadhyaya, Ex-Director, NAL and Mr. M. K. Sridhar, Head, MT for the support. They acknowledge the help of K. J. Prashanth, Harish Barshilia, A. Vanaja, K. Venkataramaiah, and A. Sri Ganesh for the help in experiments.

## References

- [1] H. Kawai, "The piezoelectricity of poly(vinylidene fluoride)", *Jpn. J. Appl. Phys.*, (1969), 8, pp. 975-977.
- [2] R.G. Kepler, and R.A. Anderson, "Ferroelectric polymer", *Adv. Phys.*, (1992), 41(1), pp. 1-57.
- [3] J.G. Bergman, J.H. McFee, and G.R. Crane, "Pyroelectricity and optical second harmonic generation in polyvinylidene fluoride films", *Appl. Phys. Lett.*, (1971), 18(5), pp. 203-203.
- [4] G. Guerra, G.D. Dino, R Centore, V. Petraccone, J. Obrzut, F.E. Karasz, and W.J. MacKnight, "Structural characterization of vinylidene fluoride/vnyl fluoride copolymers", *Macromol. Chem. Phys.*, (1989), 190(9), pp. 2203-2210.
- [5] J.B. Lando, and W.W. Doll, "The polymorphism of poly(vinylidene fluoride) the effect of head-to-head structure", *J. Macromol. Sci. Phys.*, (1968), 2(2), pp. 205-218.
- [6] A.J. Lovinger, T. Furukawa, G.T. Davis, and M.G. Broadhurst, "Crystallographic changes characterizing the Curie transition in three ferroelectric copolymers of vinylidene fluoride and trifluoroethylene: 1. As-crystallized samples", *Polymer*, (1983), 24, pp. 1225-1232.
- [7] K. Tashiro, and H.S. Nalwa, "Ferroelectric Polymers: Chemistry, Physics, and Applications", *Ferroelectr. Polym.*, (1995), pp. 63-181.
- [8] T. Furukawa, "Ferroelectric properties of vinylidene fluoride copolymers", *Phase Transitions*, (1989), 18, pp. 143-211.
- [9] E. Bellet-Amalric, and J. F. Legrand, "Crystalline structures and phase transition of the ferroelectric P(VDF-

- TrFE) copolymers, a neutron diffraction study”, *Eur. Phys. J.*, (1998), 3, pp. 225-236.
- [10] A.J. Lovinger, T. Furukawa, G.T. Davis, and M.G. Broadhurst, “Crystallographic changes characterizing the Curie transition in three ferroelectric copolymers of vinylidene fluoride and trifluoroethylene oriented or poled samples”, *Polymer*, (1983), 24, pp. 1232-1239.
- [11] K. Henkel, I. Lazareva, D. Mandal, I. Paloumpa, K. Müller, Y. Koval, P. Müller, and D. Schmeiber, “Electrical investigations on MFIS structures using P(VDF/TrFE) as ferroelectric layer for organic non-volatile memory applications”, *J. Vac. Sci. Technol.*, (2009), 27, pp. 504.
- [12] Cheng Huang, R. Klein, Feng Xia, Hengfeng Li, and Q.M. Zhang, “Poly(vinylidene fluoride-trifluoroethylene)-based high performance electroactive polymers”, *IEEE Trans. Dielectr. Electr. Insul.*, (2004), 11, pp. 299-311.
- [13] A. George Samara and Francois Bauer, “The role of high pressure in the study and applications of the ferroelectric polymer polyvinylidene fluoride and its copolymers” *Ferroelectrics*, (1995), 171, pp. 299-311.
- [14] R.A. Graham, M.U. Anderson, F. Bauer, and R.E. Setchell, “Shock Compression of Condensed Matter”, *J. Appl. Phys.*, (1991), pp. 883.
- [15] Mengjun Bai and A.V. Sorokin, “Determination of the optical dispersion in ferroelectric vinylidene fluoride (70%)/trifluoroethylene (30%) copolymer Langmuir–Blodgett films”, *J. Appl. Phys.*, (2004), 95(7), pp. 3372-3377.
- [16] J. Choi, C.N. Borca, P.A. Dowben, A. Bune, M. Poulsen, S. Pebley, S. denwalla, S. Ducharme, L. Robertson, V. M. Fridkin, S.P. Palto, N.N. Petukhova, and S.G. Yudin, “Phase transition in the surface structure in copolymer films of vinylidene fluoride (70%) with trifluoroethylene (30%)”, *Phys. Rev.*, (2000), 61(8), pp. 5760-5770.
- [17] V. Sencadas, G.R. Filho, and S. Lanceros-Mendez, “Processing and characterization of a novel nonporous poly(vinylidene fluoride) films in the  $\beta$ -phase”, *J. Non-Cryst. Solids*, (2006), 352, pp. 2226-2229.
- [18] Li. “Electron emission from ferroelectric copolymer thin films of vinylidene fluoride and trifluoroethylene”, *Appl. Phys. Lett.*, (2006), 89, pp. 222907.
- [19] D. Duo Mao, M.A. Quevedo-Lopez, H. Stiegler, H.N. Alshareef, and B.E. Gnade, “Optimization of poly(vinylidene fluoride-trifluoroethylene) film as non-volatile memory for flexible electronics”, *Org. Electron.*, (2010), 11(5), pp. 925.
- [20] Q.M. Zhang, Vivek Bharti, and X. Zhao, “Giant electrostriction and relaxor ferroelectric behavior in electron-irradiated poly(vinylidene fluoridetrifluoroethylene) copolymer”, *Science.*, (1998), 280, pp. 2101-2104.
- [21] Th. H. De Keijsers, J.I. Langford, E.J. Mittemeijer, and A.B.P. Vogels, “Use of Voigt Function in a single-line method for the analysis of X-ray Diffraction Line Broadening”, *J. Appl. Cryst.*, (1982), 15, pp. 308-314.
- [22] Jr. R. Gregorio, and E.M. Ueno, “Effect of crystalline phase, orientation and temperature on the dielectric properties of poly (vinylidene fluoride) (PVDF)”, *J. Mater. Sci.*, (1999), 34, pp. 4489-4500.
- [23] R. Tim Dargaville, Mathew Celina, W. Jeffrey Martin, and A. Bruce Banks, “Evaluation of piezoelectric PVDF polymers for use in space environments. Part II: effects of atomic oxygen and vacuum UV exposure”, *J. Polym. Sci., Part B: Polym. Phys.*, (2005), 43(18) pp. 2503-2513.
- [24] Kim Dong-Won, Lee Gwang-Geun, and Park Byung-Eun, “The ferroelectricity and electrical properties of P(VDF-TrFE) copolymer film”, *J. Korean Phys. Soc.*, (2007), 51(2), pp. 719-722.
- [25] K. Tashiro, K. Takano, M. Kobayashi, Y. Chatani, and H. Tadokoro, “Structure and ferro-electric phase transition of vinylidene fluoride-trifluoroethylene copolymers: 2. VDF 55% copolymer”, *Polymer*, (1984), 25, pp. 195.
- [26] M. Kobayashi, K. Tashiro, and H. Tadokoro, “Molecular vibrations of three crystal forms of poly(vinylidene fluoride)”, *Macromol.*, (1975), 8, pp. 158.
- [27] K. Tashiro, M. Kobayashi and Tadokoro, H. “Vibrational spectra and disorder–order transition of poly(vinylidene fluoride) form III”, *Macromol.*, (1981), 14, pp. 1757.
- [28] K. Tashiro, Y. Itoh, M. Kobayashi, and H. Tadokoro, “Polarized Raman spectra and LO-TO splitting of poly(vinylidene fluoride) crystal forms I”, *Macromol.*, (1985), 18, pp. 2600.
- [29] Y. Kubouchi, Y. Kumetani, T. Yagi, T. Masuda, and Nakajima, A. “Structure and dielectric properties of vinylidene fluoride copolymers”, *Pure Appl. Chem.*, 61(1), (1989), pp. 83-90.
- [30] Dipankar Mandal, K. Henkel, K. Müller, and Schmeiber, D. “Bandgap determination of P(VDF–TrFE) copolymer film by electron energy loss spectroscopy”, *Bull. Mater. Sci.*, (2010), 33(4), pp. 457-461.
- [31] Y.W. Tang, X.Z. Zhao, L.W. Helen Chad, and C.L. Cho, “Electron irradiation effects in electrostrictive P(VDF-TrFE) copolymers”, *IEEE*, (2001), pp. 793-796.
- [32] J. Clements, G.R. Davies, and I.M Ward, “A broad-line nuclear magnetic resonance study of a vinylidene fluoride/trifluoroethylene copolymer”, *Polymer*, (1992), 33, pp. 1623.
- [33] Antoine Lonjon, Lydia Laffont, Philippe Demont, Eric Dantras, and Colette Lacabanne, “Structural and electrical properties of gold nanowires/P(VDF-TrFE) nanocomposites”, *J. Phys. D: Appl. Phys.*, (2010), 43(34), pp. 345-401
- [34] N. Murayama, K. Nakamura, H. Obara, and M. Segawa, “The strong piezoelectricity in polyvinylidene fluoride (PVDF)”, *Ultrason.*, (1976), pp. 15-22.
- [35] J.C. McGrath, L. Holt, and D.M. Jones, “Recent measurements on improved thick film piezoelectric PVDF polymer materials for hydrophone applications,” *Ferroelectrics*, 50, (1983), pp. 13-20.
- [36] B. Mohammadi, A.A. Yousefi, and S.M. Bellah, “Effect of tensile strain rate and elongation on crystalline structure and piezoelectric properties of PVDF thin films”, *Polym. Test.*, 26, (2007), pp. 42-50.
- [37] Bobby, Piezo Film Sensors Technical Manual. (2011),
- [38] V.T Rathod, Mahapatra, D.Roy., Anjana Jain, and A. Gayathri, “Characterization of a large area PVDF thin film for electro-mechanical and ultrasonic sensing applications”, *Sens. Actuators, A.*, (2010), 163(1), pp.164-171.